Available online at www.sciencedirect.com
SCIENCE DIRECT®
Physica E 19 (2003) 240–245
PHYSICA E
www.elsevier.com/locate/physe

Controlled domain wall motion in micron-scale permalloy square rings

A. Imre[a], G. Csaba[a,*], V. Metlushko[b], G.H. Bernstein[a], W. Porod[a]

[a] Center for Nano Science and Technology, Department of Electrical Engineering, University of Notre Dame, Notre Dame, IN 46556, USA
[b] Department of Electrical Engineering and Computer Science, University of Illinois, Chicago, IL 60607, USA

Abstract

Domain configurations and magnetization reversal processes of two-micron size permalloy square rings are investigated. We demonstrate that such rings display a few distinct domain structures that can be transformed into each other via controlled domain wall displacement. In order to selectively control the movement of separate domain walls, we fabricated rectangular dots adjacent to the ring structure. We show that the magnetic field originating from these dots determines the evolution of the domain configurations.

Keywords: Micromagnetics; Magnetic logic devices; Magnetic QCA; Magnetization reversal

1. Introduction

Ferromagnetic behavior on the mesoscopic scale has become an intense field of research in recent years, due to both pure scientific interest and the promise of important practical applications.

Macrosize ferromagnetic samples display complex and seemingly random domain configurations. The complexity of these patterns, unfortunately, goes hand-in-hand with their irreproducibility and unpredictability. It is almost always impossible to explain an actual domain pattern with simple, qualitative arguments [1], and numerical models often fail as well.

Contrary to this, mesoscopic magnets frequently display a few well-defined domain patterns that evolve into each other at defined fields. The domain patterns can be designed by choosing a proper shape of the magnet. This offers not only a good way of testing domain theory, but gives the possibility to design actual nanomagnet devices, which work according to some pre-planned functionality. Such efforts are currently underway in the field of data storage [2,3] research and the emerging subject of magnetic logic devices [4,5].

Few-domain and single-domain structures still suffer from some unpredictability of the switching fields, due to a relatively wide distribution of nucleation fields. That is why circular rings attracted special attention recently [6]: due to the lack of strong stray fields in their flux-closure state, they show more predictable switching behavior than shapes with sharp ends.

Here, we investigate static domain structures and magnetization reversal processes of permalloy square rings. The first section introduces the fabrication process as well as describes the geometrical parameters

* Corresponding author. Tel.: +1-574-631-7850.
E-mail address: gcsaba@nd.edu (G. Csaba).

1386-9477/03/$ - see front matter © 2003 Elsevier B.V. All rights reserved.
doi:10.1016/S1386-9477(03)00323-0

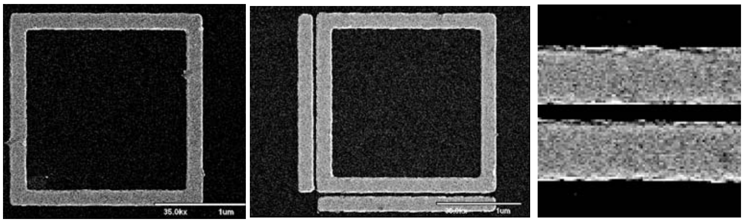

(a) (b) (c)

Fig. 1. Scanning electron micrographs of the fabricated magnetic samples: (a) is a stand-alone and (b) a controlled ring and (c) shows an approximately 300 nm × 300 nm size detail of the controlled rings.

of the sample. In the second section, we explore the static domain structures both by micromagnetic simulations and magnetic force microscopy (MFM) measurements. The next section investigates switching processes in these rings. We fabricated rectangular nanoelements next to the square rings, and we were capable of moving separate domain walls in a controlled way. This result opens up the possibility of controlling the domain wall movement in one nanoelements by a neighboring device, suggesting a way of building complex magnetic circuits from such square rings. We conclude this paper by outlining such potential applications.

2. Sample fabrication

We fabricated our square rings by standard lift-off techniques. The resist thickness was 200 nm, and the developer was MIBK:IPA:MEK (1.5%) [7]. The patterns were drawn by electron beam lithography on PMMA using a tungsten electrode at 50 kV . A 25 nm thick layer of permalloy was deposited by thermal evaporation onto the developed resist, followed by lift-off in an ultrasonic bath.

Our lithography technique routinely provides sufficient resolution for fabrication of high-quality magnetic nanostructures in the few-hundred nanometer regime.

We investigated two different structures. One of them consists of separated, 2.1 μm × 2.1 μm size permalloy square rings, as shown in Fig. 1(a).

Fig. 1(b) displays the other fabricated sample, which we will refer to as 'controlled rings'. These rings are identical to the stand-alone (uncontrolled) rings. The purpose of the neighboring rectangles is to provide a localized magnetic field that influences their switching characteristics.

These rings were subjected to a homogenous external magnetic field (of up to 4600 G) provided by an electromagnet. After applying the field, domain structures were investigated by magnetic force microscopy using a Digital Instruments Nanoscope IV atomic force/magnetic force microscope. Most investigations employed low-moment magnetic tips in order to minimize parasitic interactions between the tip and the sample.

3. Static domain configurations of a square ring

The set of basic domain configurations of square rings can be inferred from the straightforward assumption that domain walls are always pinned at the corners of the square. The walls can be either charged (when a net magnetization points inward or outward at the corner) or neutral (when the magnetization simply 'bends' at the corner). By putting domain walls with positive, negative, or zero net volume charge to the corners (and only to the corners) in all possible combinations, we obtain all theoretically possible domain configurations. These combinations are illustrated in Fig. 2.

If no charged domain walls are present in the sample, it displays a clockwise or counterclockwise ring-like magnetization distribution (see Fig. 2(a)). The next simplest configuration arrangement consists of two, oppositely-charged walls. The walls may occupy either opposite (as shown Fig. 2(b)) or neighboring corners (Fig. 2(c)); we will refer to the

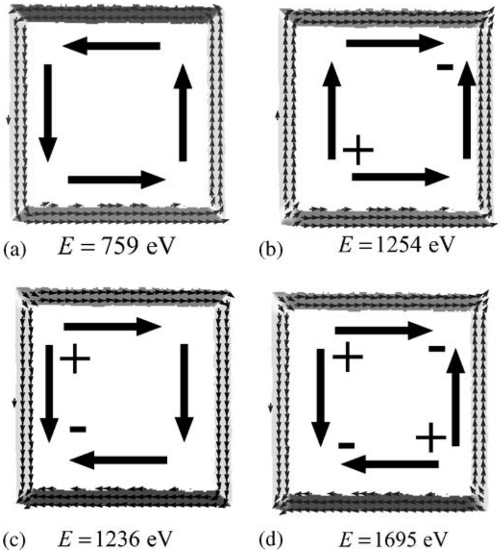

Fig. 2. Schematic of the possible domain configuration of square rings. (a), (b), (c) and (d) are schematics of the ring, diagonal, horseshoe and four domain states, respectively.

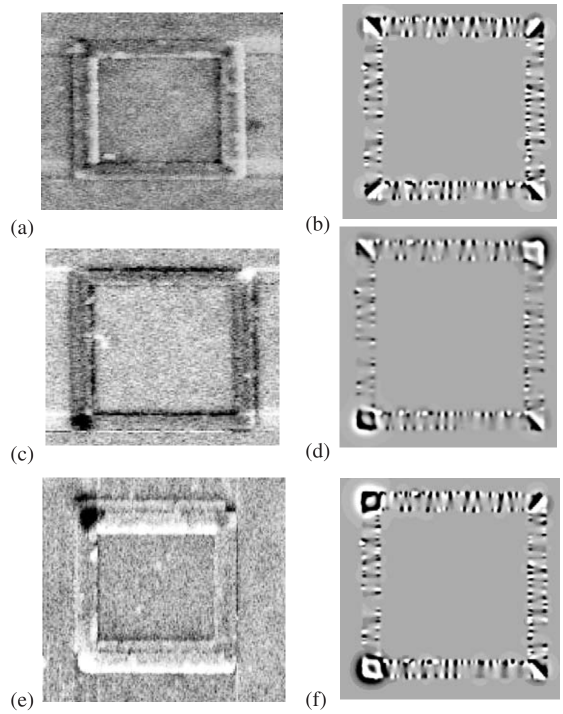

Fig. 3. Images of the possible magnetic configurations, as observed by MFM and as obtained from field calculations. (a) and (b): ring state, (c) and (d): diagonal, and (e) and (f): horseshoe.

former as ‘diagonally magnetized’ and the latter as the ‘horseshoe’ state. Putting charged domain walls at all corners yields the configuration of Fig. 2(d).

All of these configurations can be produced by micromagnetic simulations, which we performed using the OOMMF code [8]. The calculated total energies (i.e. the sum of magnetostatic and exchange energies) are also shown in Fig. 2. These numbers are consistent with the assumption that a wall with zero net charge contributes 190 eV to the total energy, while a charged wall contributes 402 eV. Most of this energy comes from the demagnetization term, while the contribution of the exchange energy is much smaller.

The zero-field degenerate ground states of the system are the two ring-like configurations. The four-domain state represents the highest energy, and it cannot be produced by a homogenous external field. Hence it is rather unlikely to appear in observations.

MFM observations confirmed the above outlined simple considerations and simulations. The most easily accessible configuration is the diagonal state, which is easily produced from any other configuration by a diagonal field larger than 500 G.

In order to confirm that the observed MFM pictures indeed correspond to the predicted domain configurations, we calculated ‘expected’ MFM images from micromagnetic simulations. It is well known that the MFM contrast is approximately proportional to the second derivative of the magnetic field above the sample [9], which can be calculated in a straight-forward manner using Maxwell’s equations. MFM contrasts of the different states—as observed and as simulated—are shown in Fig. 3.

The charged walls show up as bright or dark spots in the image, while bending of magnetization appear as fading dark-to-bright or bright-to-dark transitions. The roughness of the surface produces strong local fields, which are easily seen in the calculated images, but these patterns are averaged out in the recorded MFM images. As expected, we did not observe the four-domain state.

Higher-moment tips often caused movement of the domain walls. In the example shown in Fig. 4, the positively charged wall apparently follows the oppositely charged tip. This observation suggests that

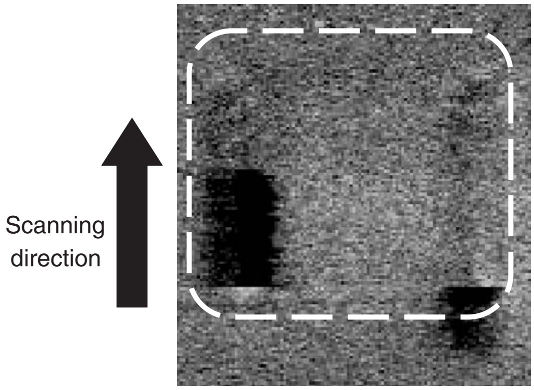

Fig. 4. The domain wall follows the oppositely charged tip in the ring. This illustrates local domain-wall manipulation by the MFM tip.

domain walls are only weakly pinned in these structures, and easily displaced. We will examine such processes in detail in the next section.

4. Domain wall displacement in square rings

The creation of domain walls requires relatively high energy, but as suggested above, their displacement involves only small fields and energies. Domain walls initially present in the structure can move and annihilate each other, forming other domain configurations.

Micromagnetic simulations and MFM observations confirm this simple, qualitative picture. The simulations of the reversal of a simple, stand-alone ring are shown in Fig. 5. The initial state in all simulations and the experiments are diagonal, two-domain states, which are the only configurations that can be reproducibly set by a homogenous applied field.

A homogenous external field parallel to the sides of the rectangle will repel one of the walls and attract the other. The walls (poles on the MFM image) are expected to flip to the opposite corners. If the rectangle were 'perfect' (domain wall pinning defects were exactly the same at the two corners), then the switching would occur in one step (i.e. at the same field). Since one of the domain walls is always pinned stronger than the other, the reversal between the two diagonal configurations occurs through an intermediate 'horseshoe state' (Fig. 5(c)).

The micromagnetic simulator code uses the shape of the magnet as input. When constructing the input field, we followed the contours of the scanning electron micrograph as closely as possible. The simulated geometry was not a perfect square, but the shape was distorted by variations introduced in the fabrication process. This resulted in a 40 G switching-field difference between the two corners. This is a reasonable estimate of the width of the corner-to-corner switching field distribution.

The measured switching field required to move the walls was 180 G, which is considerably less than the calculated value. Unfortunately, such (or even larger) discrepancies of switching-field values are not rare in micromagnetics [10]. There are two reasons to account for this discrepancy. One is that, due to limited CPU time and memory, the numerical discretization inevitably changes fine details of the simulated geometry, and this makes the modeling of pinning effects rather inaccurate. On the other hand, the OOMMF code (like most computer codes) solves the zero-temperature Landau-Lifshitz equation, and temperature fluctuations might be important in initiating the domain wall movement. Despite the disagreement between the simulated and calculated switching fields, MFM observations confirmed that the switching process proceeds as suggested by the calculations.

According to the simulations, the domain-wall sweep occurs through complicated vortex formation phenomena, as illustrated in Fig. 5(f). Nevertheless, neither the simulations nor the MFM images indicate that the details of vortex formation have visible effects on the final state.

According to the simulations, one can create the ring-like magnetic ground state in the following way: First, increase the field and reach the intermediate horseshoe state, and then do not further increase the field in the same direction, but instead apply a field along the perpendicular sides; this will cause the two charged walls to be driven towards each other and to annihilate, resulting in the ring-like state. Since we cannot foresee which of the walls moves first, we cannot tell whether the resulting ring magnetization will be clockwise or counterclockwise.

In order to gain control over the domain wall displacements, local fields should be applied that overwhelm the effect of pinning-field distributions. The simplest way of accomplish that is to fabricate

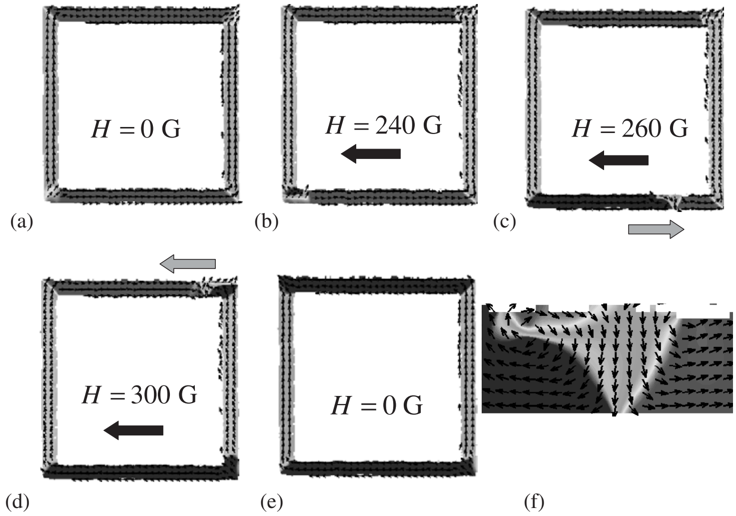

Fig. 5. Domain wall displacement initiated by a homogenous external field. Snapshots (a)–(e) are shown at different field values. (f) is a detail of the propagating wall.

magnetic elements in close proximity to the square rings such that the localized field of these nanoelements will be superimposed onto the homogenous external field.

We fabricated 2.1 μm × 180 nm rectangular nanomagnets at distances of about 40 nm from the two sides of the squares. The SEM micrograph of that structure was shown in Fig. 1(b).

After magnetizing them along their longer axis, the rectangular magnets stay in a simple and stable single domain state with two oppositely charged regions at their ends. Simple magnetostatic calculations show that the peak magnetic field generated by these rectangles at the corners of the square rings is around 200 G; this value is definitely larger than the switching-field variations.

We estimate the switching field of these rectangles (i.e., when their single-domain state is destroyed) to be approximately 300 G, which is considerably larger than the value required for domain-wall displacement in the square rings. Hence, their magnetization remains intact during the pumping field, which causes domain-wall movement, and they act solely as a 'driver' in this process, thus providing a well-localized magnetic field for the rings.

The controlled switching process, as recorded by MFM, is illustrated in Fig. 6. The initial state is the familiar diagonal two-domain configuration, plus the uniformly magnetized rectangles. There are three positively charged regions concentrated in the lower left corner. The repulsion helps to remove the wall from this corner at an applied field strength of 130 G. This pole locks to a stable location (Fig. 6(b)), and the oppositely charged other pole of the rectangle helps maintain its position. A horizontal field now moves the hitherto intact negatively charged wall, which finally annihilates with the positive one. The structure finally relaxes to a counterclockwise-rotating flux-closure domain configuration. If opposite magnetic fields were applied at each step (including the initialization), a clockwise field would result. The control elements determine which wall moves first, and such control over the final state would not be possible without these coupler elements.

Effects of dipolar coupling on the ordering of single-domain dots have been investigated recently [11–13]. However, we are unaware of any previous work demonstrating strong correlation between coupling and internal domain configuration.

5. Conclusions and potential applications

This paper investigated micron-scale ferromagnetic square-ring structures, and demonstrated how

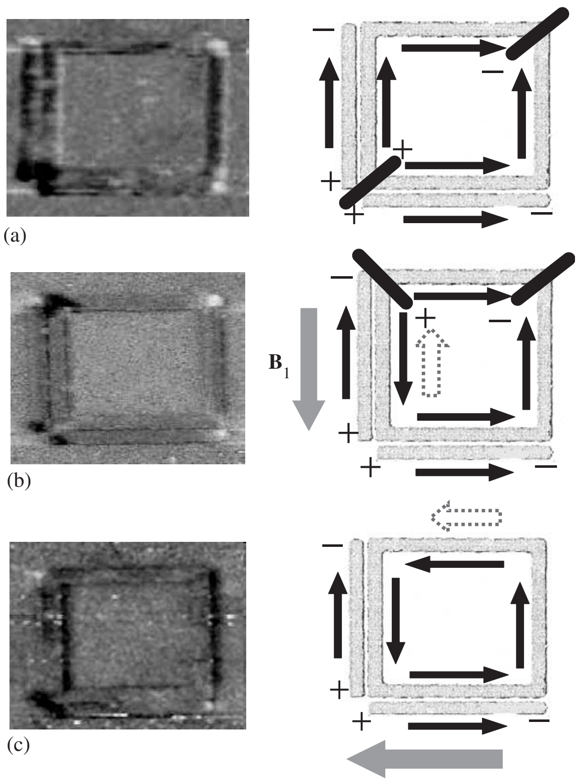

Fig. 6. Controlled domain-wall displacement, as recorded by MFM. An initial (diagonal) configuration (a) switches to a horseshoe state (b) and the walls of this horseshoe finally annihilate, forming a ring configuration (c). The coupler elements control which wall sweeps. The schematics on the right help the interpretation of the images.

external field pumping and coupling to adjacent magnetic dots can be used to control their domain configurations. Such square rings and similar few-domain structures opens up the possibility of designing particular 'functional' domain structures, i.e. domain patterns that are particularly useful for certain applications. This is especially promising in the light of recent proposals [4,5] suggesting that such nanomagnets might be applied as building blocks of signal processing devices. In these proposed structures, propagating domain walls and/or magnetic coupling transmit information between the building blocks, which can be single-domain or few-domain structures. Precise control over simple domain configurations is an essential requirement for the successful operation of such a device concept.

We presented an example of such control on a simple micromagnetic system, namely square rings coupled to rectangular magnets. We have shown experimentally and theoretically that these rings can display a few qualitatively straightforward domain configurations, which can be transformed into each other via properly designed external field pulses. The rings can be designed in such a way that uncontrollable deviations from the perfect shape play little role in their operation.

Further research should answer the question whether much more complicated and still well-controlled structures can be built from such ring-like magnets, and whether they can produce the desired complex functionality.

Acknowledgements

This work was supported in part by grants from the Office of Naval Research, the National Science Foundation, and the W.M. Keck Foundation.

References

[1] A. Hubert, R. Schafer, Magnetic Domains, Springer, Berlin, 1998.
[2] G.A. Prinz, Science 282 (1998) 1660.
[3] C.A. Ross, H.I. Smith, T. Savas, M. Schattenburg, M. Farhoud, M. Hwang, M. Walsh, M.C. Abraham, R.J. Ram, J. Vac. Sci. Technol. B 17 (1999) 3168.
[4] D.A. Allwood, Gang Xiong, M.D. Cooke, C.C. Faulkner, D. Atkinson, N. Vernier, R.P. Cowburn, Science 296 (2002) 2003.
[5] G. Csaba, W. Porod, J. Comput. Electron. 1 (2002) 87.
[6] J. Rothman, M. Kläui, L. Lopez-Diaz, C.A.F. Vaz, A. Bleloch, J.A.C. Bland, Z. Cui, R. Speaks, Phys. Rev. Lett. 86 (2001) 1098.
[7] G.H. Bernstein, D.A. Hill, W.P. Liu, J. Appl. Phys. 71 (8) (1992) 4066.
[8] M.J. Donahue, Porter DG OOMMF User's Guide, Version 1.0, Interagency Report NISTIR 6376. Online: http://math.nist.gov/oommf/.
[9] D. Sarid, Scanning Force Microscopy: with Applications to Electric, Magnetic, and Atomic Forces, Oxford University Press, New York, 1994.
[10] A. Aharoni, J. Magn. Magn. Mater. 203 (1999) 33.
[11] R.P. Cowburn, M.E. Welland, Science 287 (2000) 1466.
[12] R.P. Cowburn, Phys. Rev. B 65 (2002) 092409.
[13] H. Koo, M. Dreyer, V.V. Metlushko, R.D. Gomez, IEEE Trans. Magn. 37 (4) (2001) 2049.